The Realization of a Lossy Material with a Prescribed Transparency Window in the Bulk.
ARO Grant # DAAD19-99-1-0351
Final Progress Report
Date November 23, 2000

1.0 Foreword:

The research in this project addresses the issue of antenna proliferation. Whenever a multiplicity of antenna functions such as communications, intelligence, direction finding, and electronic warfare, must operate on a single platform, the need to isolate the antennas and their signals from each other becomes a performance-limiting problem. The only solution available today is to employ frequency-selective surfaces and solids (so-called Photonic Band Gap materials). These are carefully structured periodic arrangements of conducting or dielectric elements that create stopbands in their transmission functions at specific frequencies and angles. However, by definition these require complex manufacturing approaches with exacting tolerances, and they suffer from out-of-band grating lobes. The ideal solution to this packaging problem would be the existence of a bulk material that is only transparent at a prescribed frequency. Such a material would allow antennas operating at different bands to share "real estate" with a minimum of mutual coupling. It would also allow the construction of frequency selective radomes with no out-of-band grating lobes. The proof that such a material can be constructed, with a tuned electromagnetic window obtained in the bulk through chemical means, is the subject of this research.

2.0 Table of Contents:

REPORT DOCUMENTATION PAGE

Form Approved
OMB NO. 0704-0188

1. AGENCY USE ONLY (Leave Blank)	2. REPORT DATE December 5, 2000	3. REPORT TYPE AND DATES COVERED FINAL 09/01/99 through 10/31/00

4. TITLE AND SUBTITLE
The realization of a lossy material with a prescribed transparency window in the bulk.

5. FUNDING NUMBERS
Grant #DAAD19-99-1-0351

6. AUTHOR(S)
Rodolfo E. Diaz and William Glaunsinger

7. PERFORMING ORGANIZATION NAME(S) AND ADDRESS(ES)
Arizona State University, Office of Research and Creative Activities
P.O.Box 871603
Tempe, AZ 85287-1603

8. PERFORMING ORGANIZATION REPORT NUMBER

9. SPONSORING / MONITORING AGENCY NAME(S) AND ADDRESS(ES)
U. S. Army Research Office
P.O. Box 12211
Research Triangle Park, NC 27709-2211

10. SPONSORING / MONITORING AGENCY REPORT NUMBER
ARO 40179.1-EL

11. SUPPLEMENTARY NOTES
The views, opinions and/or findings contained in this report are those of the author(s) and should not be construed as an official Department of the Army position, policy or decision, unless so designated by other documentation.

12 a. DISTRIBUTION / AVAILABILITY STATEMENT
Approved for public release; distribution unlimited.

12 b. DISTRIBUTION CODE

13. ABSTRACT (Maximum 200 words)

(A) Specific Aims: The first phase of this project consists of the period 9/1/99 to 12/31/00 being reported here. The goal consists of two steps: (1) To prove the existence of Lorentz resonant dielectrics in the microwave range by measuring the X-band frequency dependent complex permittivity of stable metal-ammonia solutions. (2) To prove experimentally that such resonances can be used to create a transparency window in the spectrum.
(B) Results:the presence of a sharp Lorentz resonance in the permittivity at 9GHz was proven in tests of capillaries of the selected solution (LiNH3). Its behavior was modelled in terms of a background ionic solution with metallic clusters in which a second resonant species co-exists. Because the liquid-filled capillary constitutes an inductive obstacle in the waveguide, the Lorentz resonance had the effect of suddenly educing the total power absorbed at its frequency. In other words, the test set-up exhibited the transparency window effect.
(C) Plans for next reporting period: Recommendations were made for initiating the next phase with further chemical experiments to determine the range of control available to move the resonant frequency by substituting alternate alkali or bivalent metals. Success in that area will leave us with a robust model of the resonant properties of these solutions that can then be used to find or synthesize other microwave resonant materials. The next phase of the project is an optional phase where these results are applied to the development of a solid material exhibiting this property of chemically tuned resonance.

14. SUBJECT TERMS
Frequency-selective materials, Lorentz resonance, microwave dispersive permittivity liquid metal-ammonia solutions

15. NUMBER OF PAGES
20

16. PRICE CODE

17. SECURITY CLASSIFICATION OF REPORT	18. SECURITY CLASSIFICATION ON THIS PAGE	19. SECURITY CLASSIFICATION OF ABSTRACT	20. LIMITATION OF ABSTRACT
UNCLASSIFIED	UNCLASSIFIED	UNCLASSIFIED	UL

3.0 List of Illustrations:

4.0 Statement of the Problem:

Three ingredients are required to make the tuned electromagnetic window material a reality: (1) A theory and design procedure for creating electromagnetic windows by using Lorentz resonant materials. (2) The existence of Lorentz resonant materials in the radiofrequency range. (3) A method to incorporate those materials into a composite structure.

Ingredient number one arises from the realization that because the absorption line of a sharp Lorentz resonance corresponds to extremely high conductivities, it can be used as a narrow band shield to hide the lossy elements of an absorbing composite. The counterintuitive result that an absorption band therefore results in the creation of a transparency window in a lossy material has been proven with the rigorous analysis of the case of an artificial dielectric consisting of coated resistive spheres [1]. Therefore, this proof-of-feasibility phase of the project addressed ingredient number two, the proof that useful Lorentz resonant dielectrics can exist in the radiofrequency range. This is not a trivial undertaking since most texts on the theory of dielectrics state that Lorentz resonances are dipole oscillations of atomic electron clouds and therefore limited to the Infrared and higher frequencies. (Similarly, arguments based on a two-level quantum mechanical system description also conclude that such a low frequency resonance implies a very small energy gap, easily masked by thermal noise). Furthermore, materials exhibiting Lorentz resonance behavior usually have a negative permittivity above the resonant frequency. Only plasmas and plasma-like systems have been reported with such properties in the literature, such as high Tc superconductors in the MHz range, and of course metals at optical frequencies. However, there has been evidence since the 1960's that certain metal-ammonia solutions possess a negative permittivity at X-band. In fact, in 1970, Breitsschwerdt and Radscheit [2] made microwave measurements of the real part of the permittivity of such solutions from 700 MHz to 2.5 GHz and in five waveguide bands at 6, 10, 23, 35, and 70 GHz. The reported curve (consisting essentially of six data points over two decades) strongly suggested a Lorentz resonance at 10 GHz. Therefore the work in this phase of the project focused on verifying that data in detail over the X-band range and determining whether or not that Lorentz resonance can be used to create an electromagnetic window.

Success in this phase opens the way for continuing with the project to address ingredient number three and the ultimate goal: development of the method and materials necessary to construct a tuned electromagnetic window composite.

The problems addressed in this phase included: (a) the development of the synthesis procedure and equipment for making the metal-ammonia solutions, (b) assessment of their thermal stability (since these solutions are prepared at – 78 °C), (c) design of a test set-up for measuring the dielectric properties of the highly reactive solution in the face of scant and conflicting data found in the literature, (d) implementation of the set-up for use with a network analyzer and with the capability for holding the test specimen at –40 °C, (e) development of a data analysis method for extracting the permittivity from the S parameter measurements.

5.0 Summary of the most important results.

(1) Designed and fabricated a high-vacuum apparatus for the synthesis of metal-ammonia solutions.
(2) Designed and developed special vessels and procedures for the synthesis of metal-ammonia solutions.
(3) Prepared several lithium-ammonia solutions in the concentration range 1.5-4.0 mpm, which is just on the nonmetal side of the nonmetal-metal transition.
(4) Designed and fabricated a microwave test setup and developed data-analysis techniques to extract the real and imaginary parts of the permittivity of metal-ammonia solutions.
(5) Demonstrated that lithium-ammonia solutions exhibit the desired Lorentzian resonance near 9 GHz.
(6) Demonstrated that radiofrequency Lorentz resonances are sharp enough to construct useful frequency-selective bulk materials.

Figure 1 is a plot of the power dissipated inside four capillary test specimens, a baseline containing water and three $LiNH_3$ solutions at 1.5, 2.0 and 4.0 mole percent metal. In all three metal-ammonia cases, the solutions exhibit a narrow region of reduced power dissipation around 9 GHz. Even though these solutions have a high DC conductivity, the Lorentz resonance is so sharp that it creates this partial electromagnetic window in the measurement.

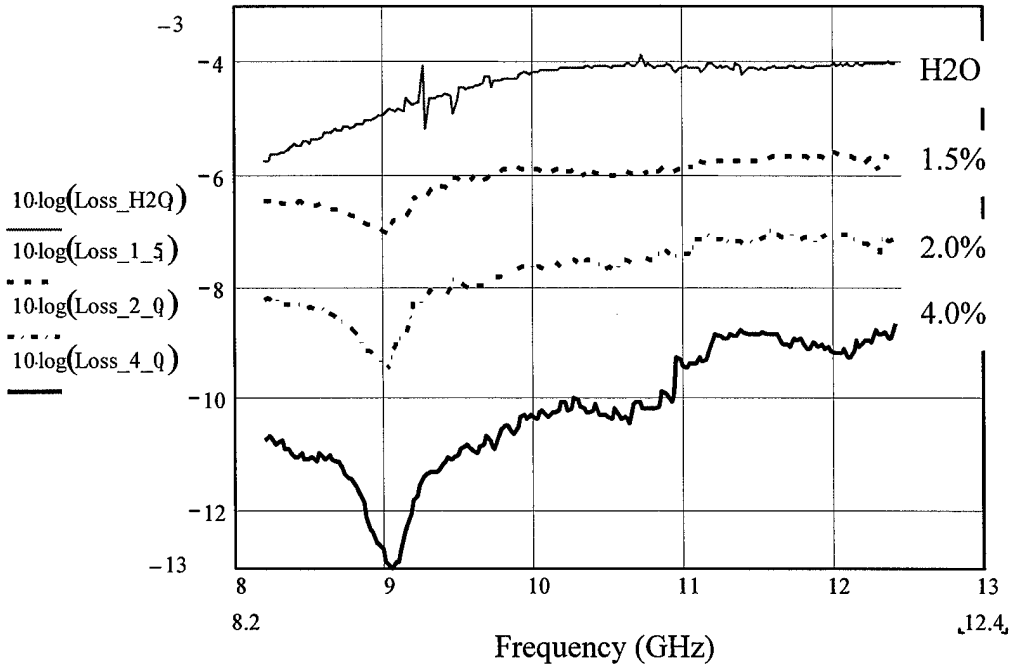

Figure 1. Power dissipated inside solution-filled capillaries, $Power_{absorbed} = 1-|S11|^2-|S21|^2$, in X-band waveguide test set-up.

Figure 2 shows the best-fit complex permittivity data consistent with the individual S11, S21 vector data and the measured dissipated power for the 4.0 mpm solution.

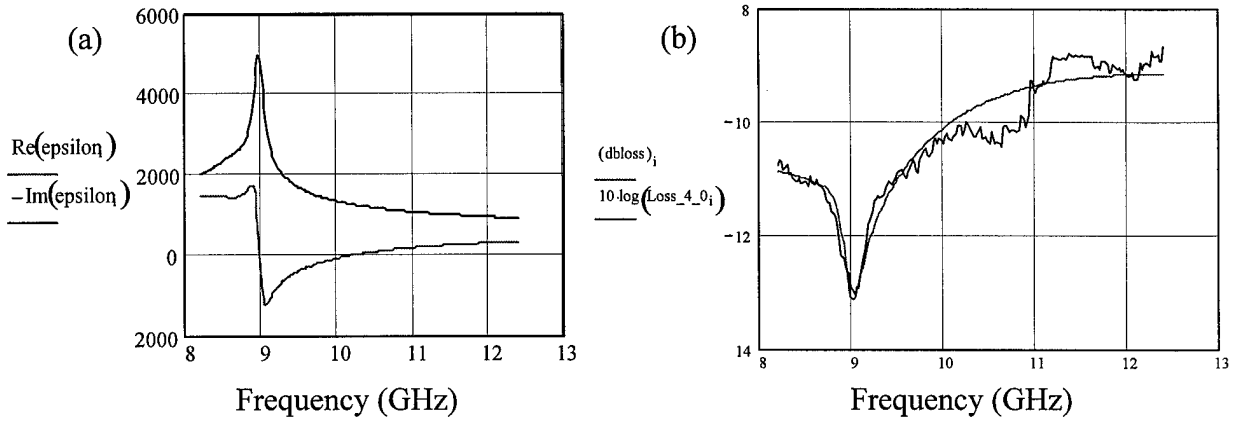

Figure 2. Analysis of the 4.0 mpm solution: (a) Best-fit complex permittivity vs frequency. (b) Calculated and measured power dissipated (dB) vs. frequency.

The data of Figure 2(a) proves the existence of sharp Lorentz resonances in the microwave range. The fact that the resonance occurs at the same frequency independent of concentration proves that they are chemically tuned. The data of Figure 2(b) proves that such Lorentz resonances can be used to create regions of reduced loss, that is, electromagnetic windows. Therefore, the feasibility phase of this project has been successfully completed.

The details of these results follow, including in section 5.1.4 an effective-medium calculation for a lossy composite showing that the Lorentz resonances found in these materials are sharp enough to create a lossy material with a prescribed transparency window in the bulk. In Section 5.1.5 we make specific recommendations regarding the next steps to be taken as we continue this work. In light of the results obtained in this phase, minor modifications to some of the details of the original plan are proposed.

5.1 Details of the Results

5.1.1 Preparation of Lithium Metal-Ammonia Solutions

The lithium-ammonia solutions investigated herein were prepared under rigorous inert conditions. All glassware used was Pyrex, cleaned in aqua regia, rinsed with distilled water followed by deionized water, and dried at 110 °C prior to use. The ammonia (99.99% electronic grade) was further purified by distilling it onto freshly cut sodium metal (99.9%) to remove any residual water or oxygen. The resulting blue sodium-ammonia solution was stored at –78 °C in a dry-ice ethanol bath. Prior to each use, the solution was frozen at –196 °C using liquid nitrogen and evacuated to remove any non-condensable gases that may be present (e.g., H_2).

The lithium-ammonia solutions were prepared using 99.9% pure lithium and transferred *in situ* to the sample capillaries used for investigation (2mm ID, 3mm OD). The reaction vessels were composed of a central (~30 ml) round-bottom flask with three legs attached at the top of the round bottom (three-legged "spider" vessels), with each leg terminated in a sample capillary. The tips of the capillaries were initially left open to facilitate cleaning and flame sealed prior to reaction vessel use. After cleaning and sealing, each vessel was evacuated to 10^{-5} Torr, with any residual surface-adsorbed water flame desorbed under dynamic vacuum. The vessels were closed

and transferred to a Vacuum Atmospheres Corp. glovebox (< 1 ppm total $O_2 + H_2O$). Li was cut to size, weighed and transferred to the central round-bottom chamber of each vessel. The reaction vessels were again closed, transferred to a diffusion-pumped vacuum manifold, and evacuated to 10^{-5} Torr. The stoichiometric amount of ammonia was distilled onto the lithium in the reaction chamber at –78 °C to create the desired solution composition to within ± 4% (e.g., the composition of a 4 mol% Li solution was 4 ± 0.16%). The reaction vessels were then closed, isolated from the vacuum manifold and immersed in a dry-ice ethanol bath to keep the entire vessel at –78 °C while transferring the solution to the capillaries. The solution was then poured into one of the three capillaries. Both the capillary and round-bottom chamber were chilled in either dry ice-ethanol or liquid nitrogen, and the capillary was flame sealed and separated from the reaction vessel. The remaining two capillaries were similarly filled and sealed. After sealing, the capillaries were stored in either dry ice-ethanol or liquid nitrogen prior to use, as prolonged exposure to ambient temperature can result in some sample decomposition. Prior to each series of measurements, the capillaries were brought to equilibrium at ambient temperature. After each study, the capillaries were returned to cold storage. The procedure was repeated for each of the Li-NH_3 solution compositions studied, with a minimum of three sample capillaries prepared for each composition. The above procedure was developed to minimize the possibility of sample decomposition that would produce lithium amide and Hydrogen gas.

5.1.2 Development of the X-band test set-up and test procedures.

The test set-up evolved during the project as we developed a better working knowledge of the solutions and the test conditions. The following discussion details our approach and findings that led to the final test set-up.

Because the work of Reference 2 was performed between –75 and – 40 °C, we assumed from the onset that it would be necessary to maintain the lithium-ammonia solutions refrigerated during testing. It is well known that these solutions are subject to decomposition at temperatures higher than – 40 °C. This fact, combined with the high reactivity in the presence of any contamination, ruled out conventional liquid dielectrometry. Since a liquid encapsulated in glass cannot touch any metal components of a transmission line or waveguide, this invalidated all test methods that require intimate contact between the test sample and the test fixture. It should be noted that in this respect we chose to deviate from the test methodology of Reference 2. According to that reference, it appears that coaxial transmission lines and waveguides were actually submerged in the test solutions. We felt that the risk of reaction on the metal walls of the waveguide was too great to guarantee that we would be measuring the pure solution and not some inhomogeneous mixture with isolated reaction sites.

Using the published data of the real part of the permittivity on one of the candidate solutions (Na-NH_3), the expected complex permittivity of the test solutions was estimated. It was determined that given the rapid change of this permittivity at X-band from insulating to conducting, the X-band skin depth of the solution would change from several millimeters to less than 1 mm. Therefore a 2mm column of the solution inserted in a waveguide would change its behavior from that of a penetrable lossy capacitive obstacle to a highly inductive one as frequency is swept. Thus it was proposed to use a 3mm OD capillary containing 2mm ID of the solution as a "shorting post" in an X-band waveguide for the basic test configuration. Measurement of the scattering parameters of the post (S11 and S12), taken with an hp8510 network analyzer, would then be inverted to yield the measured permittivity of the solution.

Thus according to this plan, to keep the solution at –40 °C, cold nitrogen gas was to be flowed through the waveguide. To minimize condensation inside the waveguide, the test section

of waveguide would be isolated from the rest of the equipment with thin Mylar windows. Figure 3 shows this original test set-up design

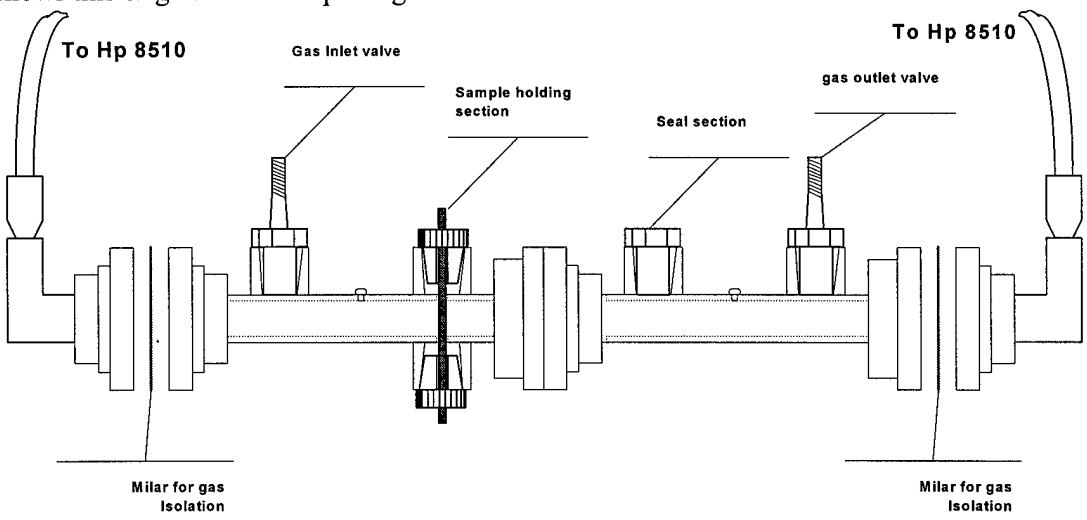

Figure 3. Original plan for a nitrogen gas cooled waveguide test set-up.

This set-up would enable us to keep the solutions cooled to –80°C by varying the rate of gas flow. The waveguide parts, capillaries and Mylar windows were procured and tested. Waveguide sections designed for pressurized operation were chosen both to facilitate the gas flow and to use one of the valve ports as a sample holder. This set-up would require portable Dewar jars to hold the liquid nitrogen and an instrumented gas-flow control system.

Before going to the trouble and expense of creating the nitrogen gas flow system, we decided to test a less expensive alternative, justified because we wanted to test the solutions at the highest possible temperature (-40 °C according to the literature). Thus the second plan called for dry ice cooling, which we estimated could get us down to –78 °C if necessary. A styrofoam container was cut to accommodate the waveguide in its interior and then filled with dry ice. The waveguide was then wrapped with a heating blanket tape and temperature controlled to achieve a constant –40 °C (on the waveguide surface). It was found that when the capillary was inserted into its valve port, the lithium-ammonia solution immediately migrated to the coldest part of the waveguide, namely the port itself, leaving a gas bubble inside the part of the capillary inside the waveguide, thus invalidating the test.

This, plus concerns about the uniformity and controllability of the temperature gradient, led us to the next modification in which the Styrofoam container was filled with a dry ice-ethanol solution. After wrapping with the heat tape, the waveguide and its cables were inserted into a plastic bag filled with ambient air and then submerged in the solution. This way the environment immediately around the waveguide was kept at a constant –55 °C. A foam cap was constructed to further insulate the valve port through which the capillary is inserted into the waveguide, as suggested in Figure 4. The Figure shows also the results of temperature measurements made at several places inside the foam cap. The goal was to ensure that the capillary would see a constant temperature over its length and thus avoid migration of the solution.

As the Figure shows, the temperature variation was kept within the range of –47 °C to –40 °C. However, access to the sample during test was severely limited.

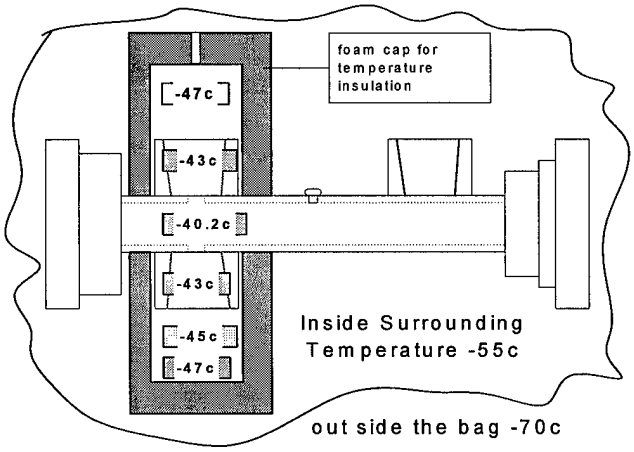

Figure 4. Temperature distribution in the submerged test set-up.

To further reduce the temperature gradient, and still permit access to the sample, the final refrigerated set-up features became:

- Placing the waveguide test set inside the foam container.
- Lining the walls and bottom of the foam container with the dry ice block.
- Not letting the dry ice make direct contact with the waveguide test set.
- The dry ice will provide the cold gas circulated inside the box.
- The cold gas has a very high temperature gradient.
- But within the foam container the gradient is minimized (isolated).
- The cold gas immediately surrounding the waveguide inside the container is at -51°C.
- The foam cap over the capillary test port kept the temperature within the cap uniform.

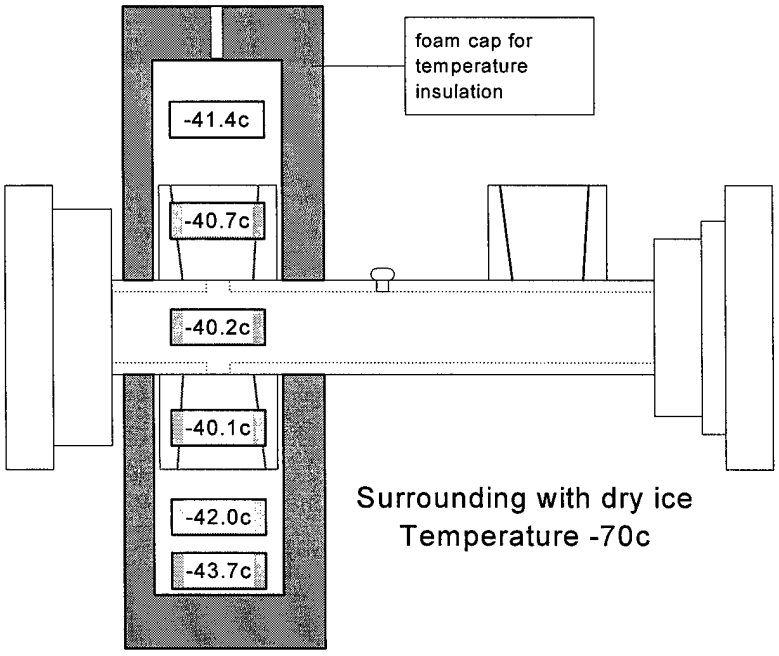

Figure 5. Temperature distribution around the capillary in the final test set-up.

This was the final set-up used for most of our low-temperature testing. In addition to the problem of solution migration in the presence of a thermal gradient, we also found that the

solutions (stored in liquid nitrogen) appeared to separate into a solid bronze-like phase and a liquid phase. Thus we were faced again with the risk of an inhomogeneous sample inside the waveguide. Variability in the test results of otherwise identical solutions suggested that this inhomogeneity was being maintained at the -40° C test temperature (due to kinetic, not thermodynamic, considerations). This finding motivated a re-evaluation of the need for a refrigerated test set-up. In the work of Thompson [3], data on the X-band negative permittivity of sodium-ammonia solutions as a function of mole percent metal shows little difference between three data sets taken at +25, 0, and -25° C. Therefore we decided to try testing at ambient temperature.

There is a risk associated with ambient-temperature testing in that once these solutions start to decompose, the decomposition progresses extremely rapidly liberating hydrogen. Therefore, the capillaries can explode due to overpressure. Given the amount of liquid in the capillaries and the thickness of the capillary walls, the strength of the explosion was assessed. It was determined that adequate protective equipment would have to be worn by the test operator, in the form of: a lab gown, gloves, and goggles. Furthermore, previous experience with these solutions indicated that if a given sealed solution is left at ambient temperature for 2 hours and it does not decompose, then it will resist decomposition for at least several days at room temperature. Therefore, after the solutions were prepared they were placed inside individual pockets in a styrofoam container and kept in a fume hood at ambient temperature for several hours. The surviving solutions were then refrigerated again in a dry ice-ethanol bath (not liquid nitrogen, to minimize phase separation) until the time for testing. For testing, the capillaries were taken out of the dry-ice ethanol bath and transported in the styrofoam box to the test lab and inserted in the test set-up at ambient temperature. A thirty-minute equilibration time was then allowed before tests were initiated.

This procedure allowed rapid testing of many solutions and it was discovered that the source of variability observed in previous tests was related to the vertical position of the capillary inside the waveguide. It was deduced that inside these thin capillaries, the solution can trap gas bubbles inside the liquid column that cannot be seen from the outside. We therefore varied the position of each capillary inside the waveguide to find the most common "signature" measurement of each solution and its two extreme deviations. Solution capillaries with a continuously varying signature as a function of vertical position were labeled as too inhomogeneous to trust. The rest of the data was taken, averaged and smoothed for analysis. The details of the analysis are given in the next section.

5.1.3 Analysis of the data.

The extreme dielectric properties of these metal-ammonia solutions made inversion of the data to extract the permittivity highly problematic. As with any non-TEM wave test set-up, there is no exact inversion. Data inversion must be performed by an optimization procedure in which a guess at the complex permittivity is inserted in the equations for calculating the reflection and transmission (S11 and S12) parameters and these are then compared with the measurements. From the difference, an error function is generated that is used to update the guess. Eventually, the guess that minimizes the error is assumed to be the correct value of the permittivity. This procedure is generally robust in the presence of moderate dielectric constants (<100). However, once the dielectric constant is extremely large (real or imaginary) it is found that there are many guesses that yield reasonably low errors. To select the correct value from among these guesses an additional requirement is imposed in the analysis, namely that the guesses at different frequencies be consistent with each other. In other words, we require that the final permittivity obtained as a function of frequency be an analytic function expandable in a series of Lorentz poles (also known

as Fosters second reactance theorem). However, the fact that the test band of frequencies is narrow (8.2 to 12.4 GHz) severely limits the application of this criterion. Nevertheless, we were able to eliminate some of the guesses using this approach. As a rule, the analysis was started with the highest frequencies and proceeded downwards in frequency, using the last guess as the initial guess for the new frequency point.

To facilitate the analysis, Marcuvitz' equivalent circuit model for the dielectric post [4] in waveguide was used to calculate the S parameters. Because the solutions have such high permittivities, we ignored the thin capillary wall and simply modeled the 2mm diameter column of liquid. It was estimated that the penalty in this assumption was a slight error in the predicted phase (that grows towards the high frequencies). To maximize the amount of data available, a shorted section of waveguide was constructed with length identical to the distance between one of the test set-up's waveguide ports and the position of the capillary. This short therefore was used as a phase calibration plane for the reflection coefficient, while a standard through calibration measurement gave the phase reference for the transmission measurement. Thus, we had full complex S11 and S12 data available for the optimization. Even so, the natural test errors associated with a real set-up introduced uncertainties. The fact that the dielectric post does not sit inside the waveguide, but penetrates its walls, introduces a small capacitive impedance into the measurements. Imperfect vertical alignment of the capillary inside the waveguide and the tolerance in the inner and outer diameter of the capillaries (less than 10%) also introduced uncertainties. These effects can be exacerbated in the presence of the very high complex permittivity of the solution under test.

The relevant equations from Marcuvitz for the centered dielectric post are:

$$\frac{jZ_a}{Z_0}+\frac{jZ_b}{2Z_0}=\frac{a}{2\lambda_g}\csc^2\frac{\pi}{2}\left[\frac{J_0(\beta)}{J_0(\alpha)}\frac{1}{\beta J_0(\alpha)J_1(\beta)-\alpha J_0(\beta)J_1(\alpha)}-S_0+\frac{\alpha^2}{4}\right]$$

$$\frac{-jZ_b}{Z_0}=\frac{\frac{2a}{\lambda_g}\left(\frac{\pi d}{a}\right)^2}{\frac{\alpha^2 J_1(\beta)}{J_1(\alpha)}\frac{1}{\alpha J_0(\alpha)J_1(\beta)-\beta J_0(\beta)J_1(\alpha)}-2}$$

$$S_0=\ln\left(\frac{4a}{\pi d}\right)-2+2\sum_{n=2}^{\infty}\sin^2\frac{n\pi}{2}\left[\frac{1}{\sqrt{n^2-\left(\frac{2a}{\lambda}\right)^2}}-\frac{1}{n}\right]$$

where the impedance Z_0 is the impedance of the fundamental TE10 mode in the waveguide, λ_g is the guided wavelength, a is the width of the waveguide (0.9" for X-band), d is the diameter of the dielectric post, J_0 and J_1 are the Bessel functions, and

$\alpha=\frac{\pi d}{\lambda},\beta=\sqrt{\varepsilon_r}\frac{\pi d}{\lambda}$, with λ = free space wavelength.

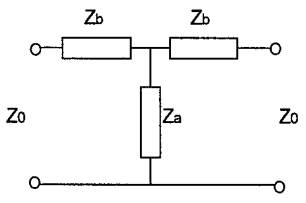

The impedances Z_a and Z_b correspond to the two-port circuit model:

As a result of the above considerations, we have four knowns, S11 and S12 magnitude and phase, and two unknowns, ε' and ε". Even though the system is over determined, the measurement tolerances still allow many possible solutions. To find a best fit to the data, we first attempt to use all four knowns. If the fit is unacceptable or non-analytic, we drop the phase information (since it is the most susceptible to test errors) and attempt to use only the magnitudes. This approach gave the initial guess at the permittivity for the solutions shown in Figure 6.

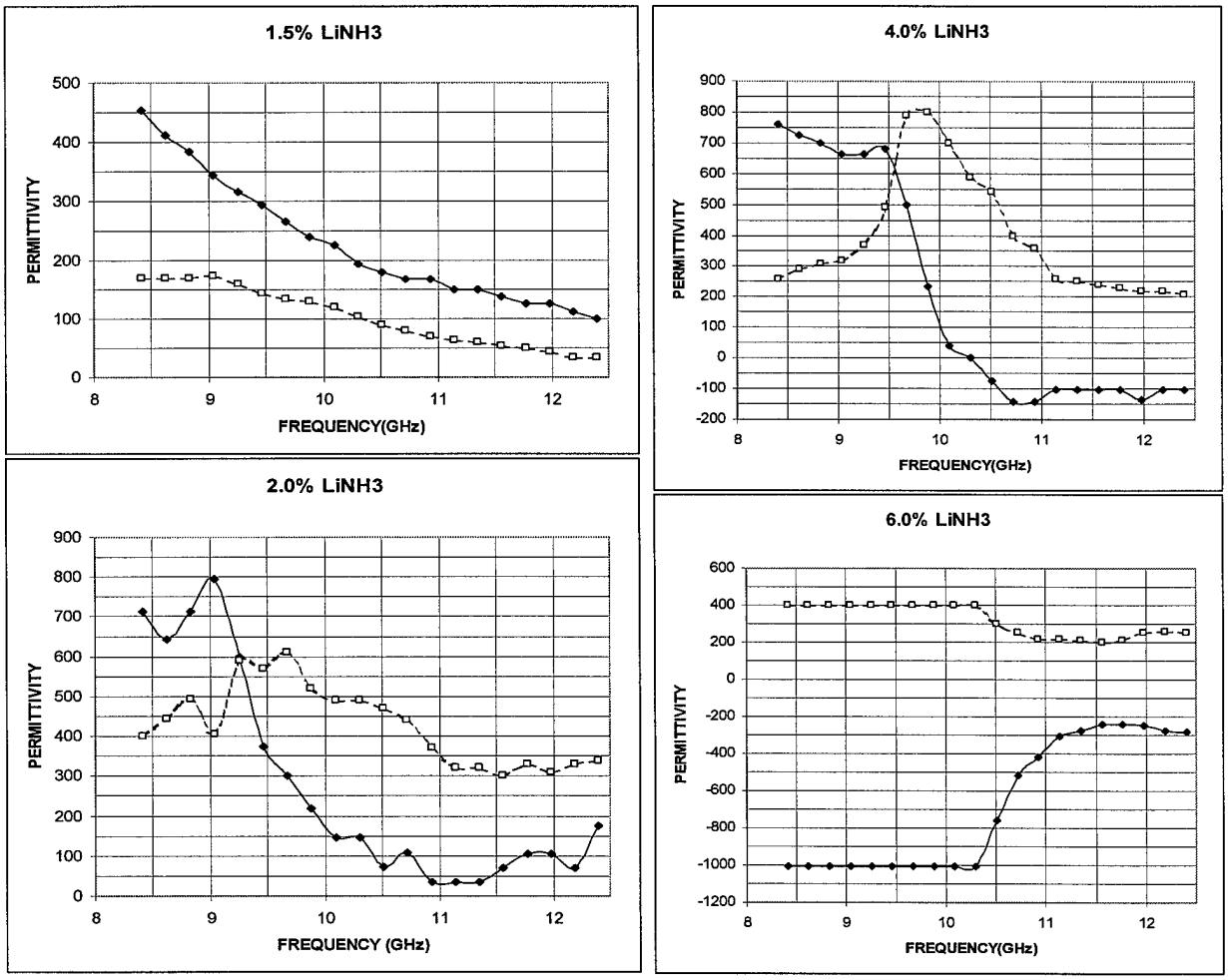

Figure 6. Initial fit of the test data obtained by minimizing independently the S11 and S12 errors. Black diamonds = real part, open squares = - imaginary part of the permittivity.

Solutions of 1.5, 2.0, 4.0 and 6.0 mpm were measured and analyzed. The method of analysis focused on obtaining the best fit to both S11 and S12 independent of each other ; that is, we sought to minimize the absolute value of the error in S11 and S12 without requiring any correlation between the two errors. The 6.0-mpm solution could only be analyzed down to 10.3 GHz. Thereafter, there was no acceptable fit. However, the trend of the data to that point suggests that the metal-nonmetal transition point had been crossed, with the real permittivity

being negative throughout the band. From this initial analysis it became clear that negative permittivities had indeed been measured and that the presence of a peak in the imaginary part around 10 GHz was suggested by the 2.0 and 4.0 mpm data. However, the extremely high permittivity at 8 GHz (somewhere between 400 and 1000) was unexpected.

Figure 7 shows our original analysis of the data from reference 2. When we first

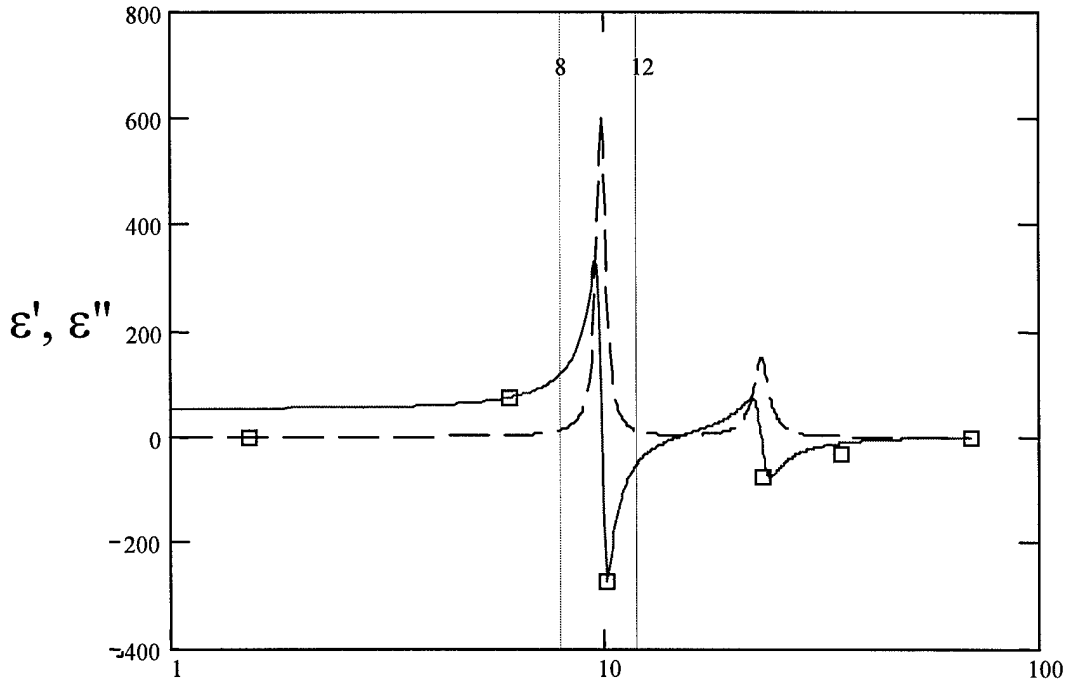

Figure 7. The best fit obtained to the six data points of reference 2. Open squares = real part data points from [2], solid line=best analytic fit to the real part, dashed = resulting - imaginary part.

analyzed this data, it was obvious that it was too scant to obtain a reliable model. However, imposing the requirement of analyticity had already shown that the low-frequency permittivity had to have been underestimated by the investigators of reference 2. In addition, there had never been any published data on the microwave conductivity of these solutions. Thus our model included no background DC conductivity, showing an imaginary part that went to zero to either side of the resonances. The initial analysis of the measured data from this project, shown in Figure 6, clearly showed an extremely high background conductivity for the solutions. Out of this background rises the Lorentz resonance.

The existence of a high imaginary part throughout the whole band motivated a re-examination of the data. It was decided that in the presence of a strong lossy scatterer, the most reliable fit to the data should not be an independent best fit to S11 and S21. Instead, the fit should take into account the sign of the error and should correlate the error in S11 with that in S12 so that the best possible fit can be obtained ***to the total power dissipated in the test***. In other words, even if the phase information is unreliable, and even if the magnitude information has test errors, the hp8510 instrument, correctly calibrated, must be able to account for the total power in the test at all times. Knowing the incident power, the reflected power, and the transmitted power, we

must always have a robust measurement of the power lost in the test, that is, dissipated into the test specimen. Indeed replotting the measured data to show the power dissipated, $1-|S11|^2-|S12|^2$, clearly showed the existence of a resonance region in all three 1.5, 2.0, and 4.0 mpm solutions. Figure 8 shows this result, and includes the result for a water-filled capillary as a baseline.

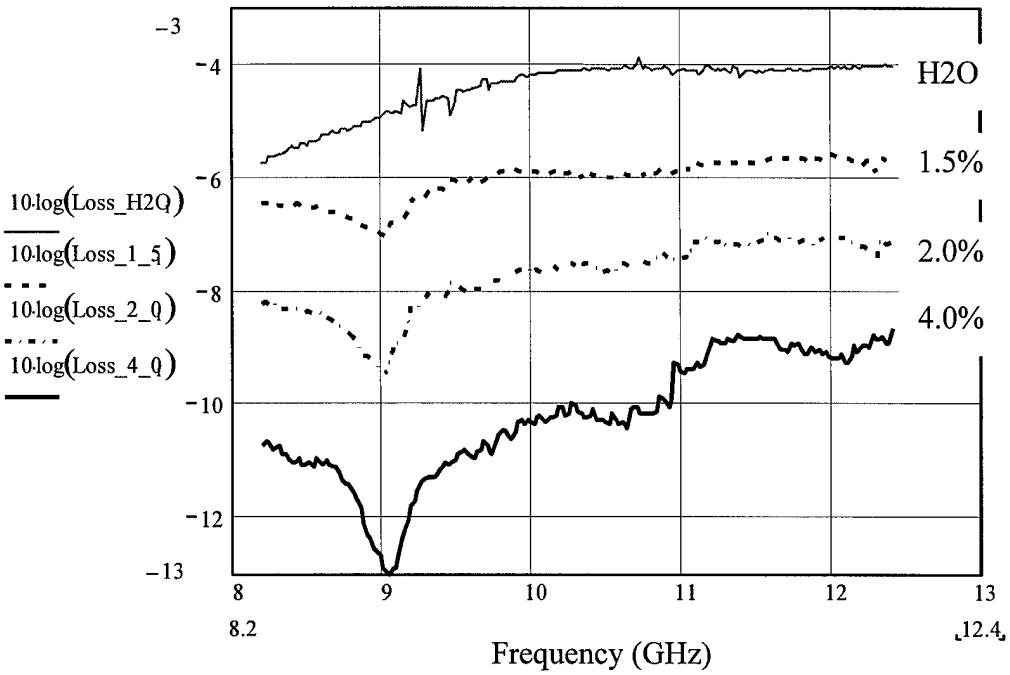

Figure 8. (Same as Figure 1) Power dissipated inside solution filled capillaries, $Power_{absorbed} = 1-|S11|^2-|S21|^2$. in X-band waveguide test set-up. The presence of a resonance region is clear near 9 GHz.

Now the data shows clearly that there is a resonant phenomenon occurring near 9 GHz for all three solutions below the metal-non metal transition. We also see the effect of the background conductivity of the solution. For the 1.5 mpm solution the average power dissipated over the band is of the order of –6dB. As more metal is added, the conductivity increases and so the scattered power increases. This actually reduces the amount of power available to be dissipated inside the solution, which is why we see the curves move downwards with increasing metal content. However, as that happens, the resonance becomes stronger and more noticeable. Based on this data, a new fit to the complex permittivity of the solutions was attempted. It was found that fitting the lost-power curve is an extremely sensitive criterion for determining the permittivity; it is sensitive both to the magnitude and the sign of the real permittivity as well as to the magnitude of the imaginary part.

Figure 9 shows the results of the fit for the 4.0 mpm solution. Figure 9(a) shows the best fit to the lost power. No attempt was made to model the detailed structure of the data above 10 GHz. Figure 9(b) shows the result of this fit (dashed lines) when compared to the measured data (solid lines) of S11 (upper solid line) and S12 (lower solid line). Figure 9(c) summarizes the error in S11, S12 and the lost power. In the region of interest, the error in the lost power was kept below 10% and the error in the reflection coefficient was always much less that 2 %, while the error in the transmission coefficient exceeded 10 % at the low frequencies. The fact that no fit

attempted could decrease the low-end error suggests that we had a systematic error in the general level of the S12 curve in this frequency range.

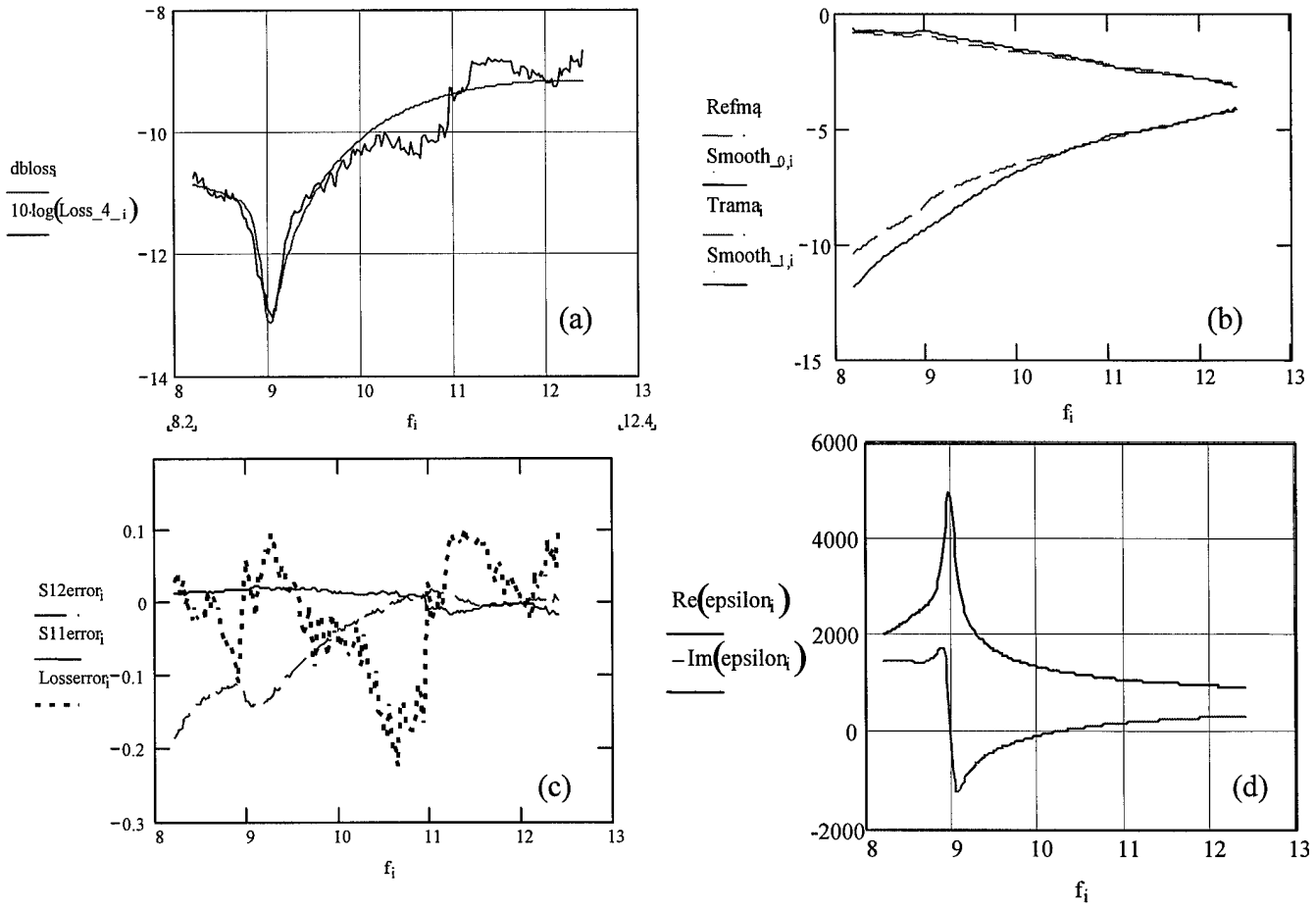

Figure 9. Best fit to the 4.0 mpm data. Fitting the resonance in lost power (dB vs. frequency) near 9 GHz (a), results in the S-parameter vs. frequency fit shown in (b) (reflection =upper curves, transmission =lower curves). The fractional error in the fit is shown in (c). The deduced complex permittivity is shown in (d).

Figure 9(d) shows the resulting estimate of the complex permittivity of this 4.0 mpm solution. It consists of a background real permittivity of the order of 550, a background conductivity of the order of 612 S/m and at least two Lorentz resonances located near 9 GHz, one much sharper than the other. The very high background real permittivity may have its origin in localized metallic clusters. That is, a microscopic inhomogeneity in the solution where the nonmetal-to-metal transition occurs in isolated pockets would lead to the creation of an artificial dielectric, magnifying the natural permittivity of ammonia (30) many fold. This process would be consistent with a percolation-like approach to the nonmetal-to-metal transition point occurring somewhere between 4.0 and 6.0 mpm. (The possibility that such inhomogeneity is fostered or enhanced by confining the solution to a thin capillary cannot be discounted.) The high background conductivity is consistent with DC conductivity measurements reported in [5]. Therefore, it is concluded that the properties of this solution can be understood in terms of the behavior of two species:

The first is a mixture of metallic clusters in a background ammonia solution with ionic and solvated electron conduction, and the second is another species exhibiting strong resonant

behavior around 9 GHz. Proving the existence of this second species was one major goal of this feasibility phase of the project.

To finish validating this model, the data for the 1.5 mpm solution was similarly analyzed. Figure 10 shows that the worst case error is of the order of 8% in the transmission coefficient, less than 2% for the reflection coefficient, and within 6% for the lost power. The deduced complex permittivity now shows a more subtle effect from the resonance.

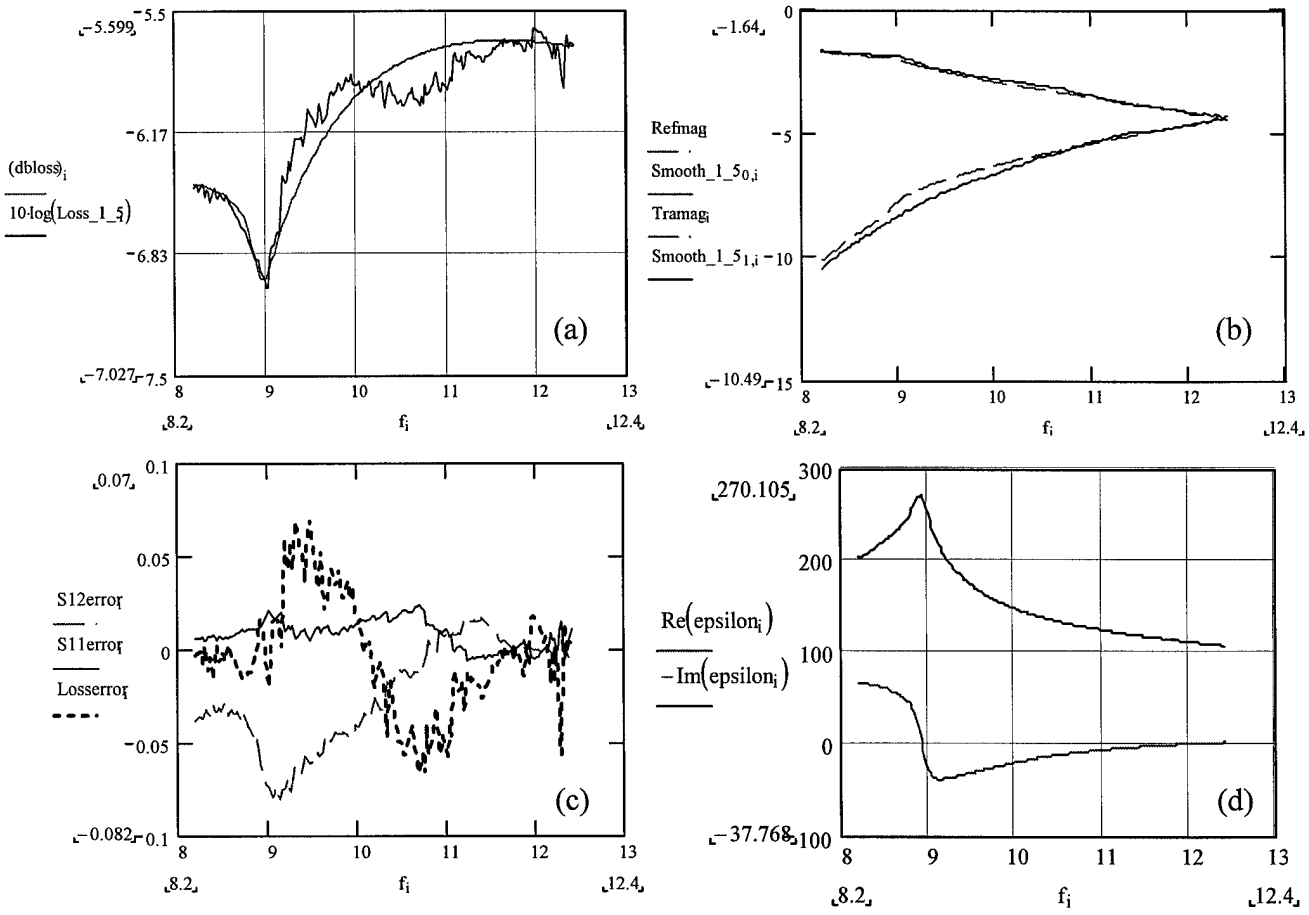

Figure 10. Best fit to the 1.5mpm solution data. Fitting the resonance in lost power near 9GHz (a), results in the fit shown in (b) to the reflection (upper curves) and transmission (lower curves) coefficients. The error in the fit is shown in (c). (d) The deduced complex permittivity.

For this case, it is found that the background permittivity of the 1.5 mpm is 15 (as opposed to 550 for the 4.0 mpm), the background conductivity is of the order of 72 S/m (as opposed to 612 S/m for the 4.0 mpm solution). These results are consistent with the model that the first species in this solution is a mixture of metallic clusters. At 1.5 mpm, they are far from percolation and their effect on the background is greatly reduced. Again two Lorentzians were enough to model the sharp drop in lost power. It is hypothesized that they must model the two extremes of a continuum of resonances near 9 GHz, associated with the second species.

The Lorentzians used to model the resonance near 9 GHz also change their character in going from 4.0 mpm to 1.5 mpm. Figure 11 shows the two model resonances for the 4.0 mpm solution, while Figure 12 shows the model for 1.5 mpm.

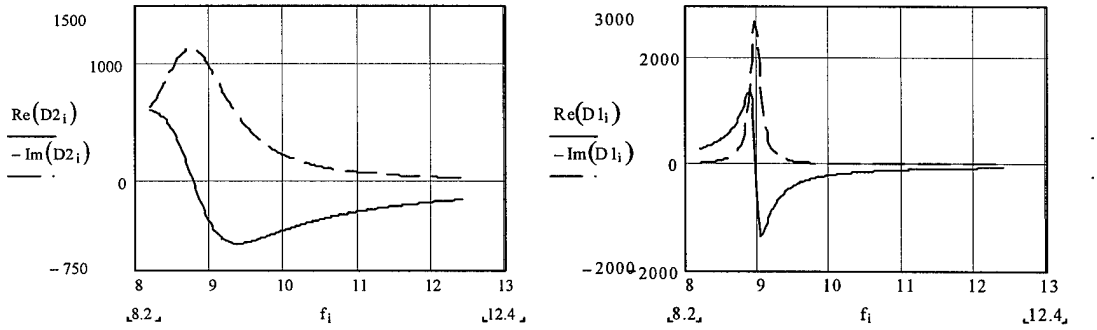

Figure 11 . Complex permittivity (real= solid, -imaginary=dashed) vs. frequency plots showing the two resonances used to model the sudden drop in lost power near 9 GHz in the 4.0 mpm solution. These probably represent two extremes of a continuum of tightly coupled resonances creating the sharp rise in imaginary permittivity at this frequency.

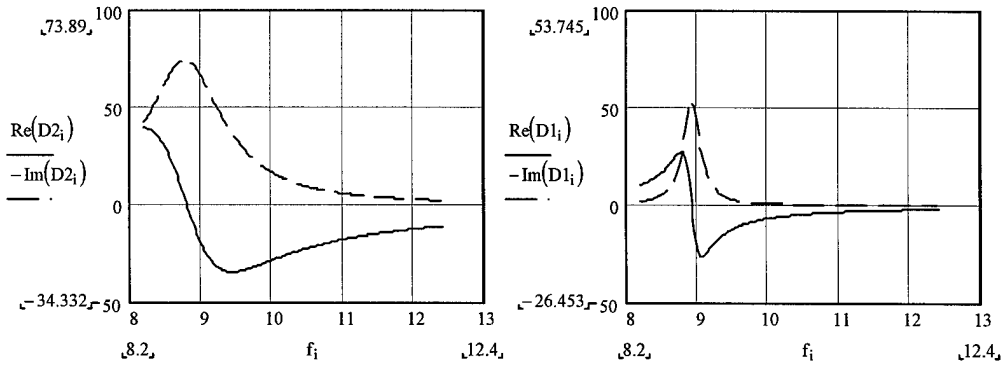

Figure 12. The two resonances used to model the sudden drop in lost power near 9 GHz in the 1.5 mpm solution.

The Table below summarizes the parameters of the best-fit models for the 1.5, 2.0 and 4.0 mpm solutions, where the equation for a Lorentzian is written in the form:

$$\varepsilon(f) = \frac{A}{1 + i\left(\frac{f}{f_{rlx}}\right) - S\left(\frac{f}{f_{rlx}}\right)^2}$$, A= Amplitude, S= Sharpness, f_{rlx}=relaxaton frequency

mpm	Background ε relative	Background σ (S/m)	Ampl. 1st Lorentzian	Sharpness	Ampl. 2nd Lorentzian	Sharpness
1.5	15	72	11	45	1.7	1000
2.0	200	222	27	48	10	1700
4.0	550	612	160	50	50	3000

The "sharpness" is the ratio of the inductive to the capacitive time constant in the LRC (inductor-capacitor-resistor) model of the Lorentz resonance.

In conclusion, it has been demonstrated that sharp Lorentz resonances in the permittivity function can exist in the radiofrequency range. The lithium-ammonia solution exhibits such a resonance near 9 GHz. We hypothesize that the complete behavior of these solutions can be understood in terms of two species: The first, behaves as a mixture of metallic clusters in an ionic solution that is approaching percolation. These metallic clusters may consist of coordinated regions of various sizes where the number of metal ions exceeds that of the ammonia moldecules, leading to high conductivity. It would be expected that to exist, these metallic clusters must exceed a critical size. Clusters in which there is no excess metal would be expected to be insulating and contribute to the background permittivity. The increase in solution background conductivity and background permittivity with increasing mole percent metal fraction is consistent with percolation models in which the correlation length of the metallic cluster size grows rapidly (and without bound, in the limit) as the percolation threshold is approached.

The second species is highly resonant at a precise frequency, independent of concentration. In our model, the two Lorentzians are used to represent a possible spectrum of Lorentz resonances located in the immediate vicinity of 9 GHz. The fact that the sharpness of the resonances is affected by the concentration of the solution, suggests that this second species is "loaded" by the presence of the first species. Nevertheless, the fact that they do not move away from 9 GHz makes it clear that these Lorentz resonances are chemically and not physically controlled. This is a key finding for continuing with this project. If we can isolate the resonant species and understand the mechanism by which it resonates at 9 GHz, we should be able to create new species resonating at other chemically prescribed frequencies. The usefulness of these sharp resonances are explored in the next section.

5.1.4 Proof of the utility of these resonances.

If the resonant species of these solutions or other similar systems can be isolated and implemented as a coating on resistive particles, the effects predicted in [1] can be realized. Thus, for this example we limit ourselves to the case of a plastic host solution of permittivity 3.0 to which are added resistive spheres coated with a layer of the resonant medium. An effective-medium model that closely matches the predictions of [1] is obtained by calculating the effective polarizability of the coated spheres using the Reverse Mossotti expression, and then calculating the effect of these spheres in the host by using the Clausius-Mossotti expression (see [6]). Figure 13 shows the results for the following scenarios:

(a) 20% volume fraction of spheres of conductivity 8 S/m coated with a layer 0.08 radii thick of a material with the sharp Lorentz resonance of Figure 11. The result is a material with 1 dB/inch loss at 9 GHz and then having a sharp rise in its insertion loss at all higher frequencies.
(b) 20% volume fraction of lossless dielectric spheres of permittivity = 4 coated with a layer 0.01 radii thick of the same resonant material. Now we have a stopband filter at 9 GHz.
(c) 10% volume fraction of spheres of conductivity 4 S/m coated with a layer of the resonant material containing both broad and sharp resonances of Figure 11. Now we have a low-pass filter with 0.5 dB/in loss below 9 GHz and more than 15 dB/in above.
(d) Moving the sharp resonance to 12 GHz creates a material with 1 dB/in insertion loss at 9 GHz, 6dB/in at 7 GHz and again much higher loss for all frequencies higher than 9 GHz.

Sharper windows than in cases (a) and (d) above can be created by using elongated particles instead of the spheres assumed in this exercise. The object of these calculations was simply to show that a tuned Lorentz material with the realistic properties measured in these metal-ammonia solutions can be used to create a variety of new frequency-selective composites that can either pass or block a band of frequencies. This property would be intrinsic to the bulk of the composite and would place no restriction on the shape that the composite can take.

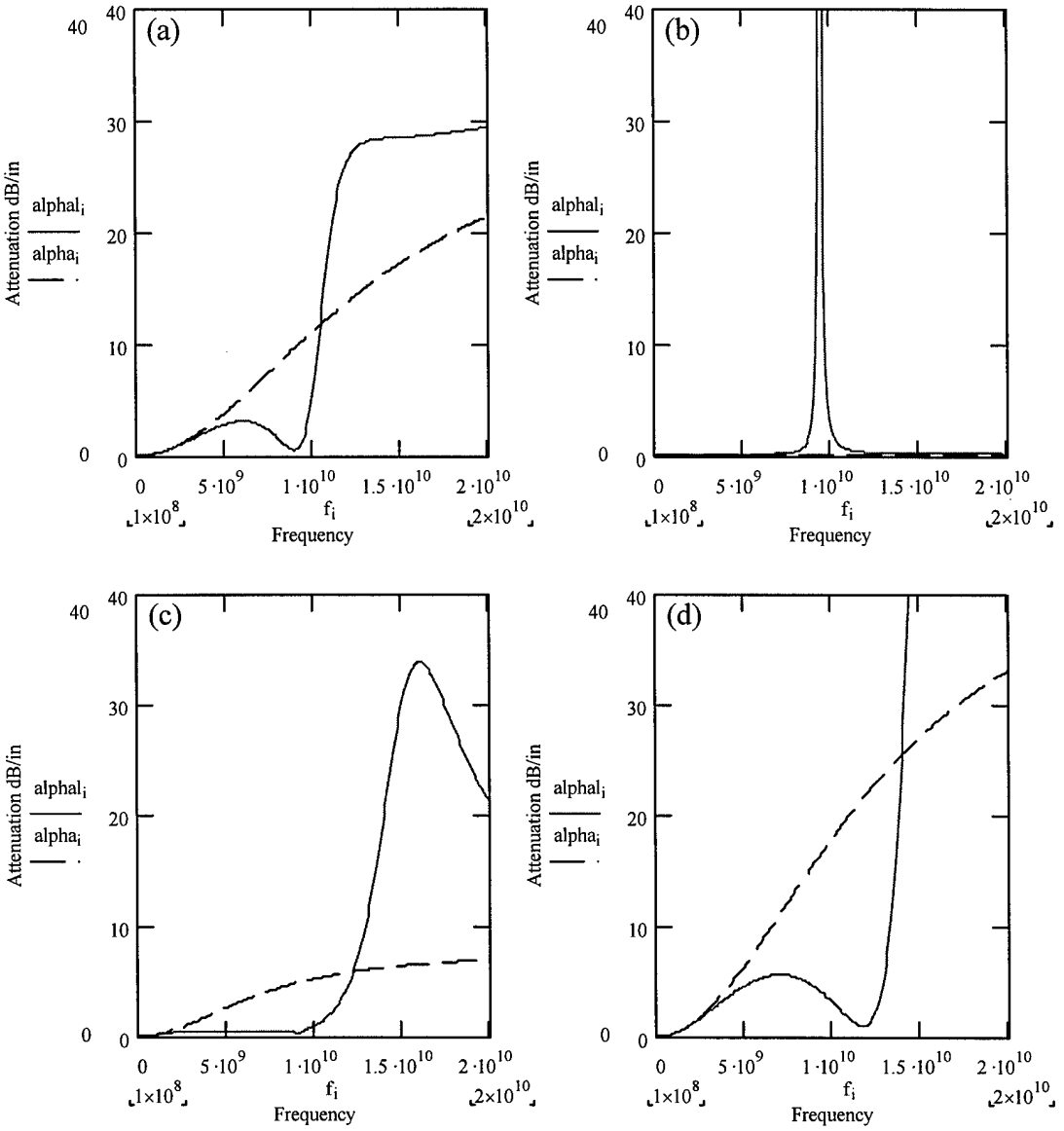

Figure 13. Attenuation constant of various composites consisting of (lossy) dielectric spheres coated with a thin layer of Lorentz resonant material with the properties of Figure 11. Dashed curve is for the material with uncoated spheres.

5.1.5 Concluding remarks and the next step.

Success in this phase opens the way for continuing with the project to address the ultimate goal: development of the method and materials necessary to construct a tuned electromagnetic window composite. In addition to proving that materials with Lorentz resonances in their radiofrequency permittivity can exist, we have developed a first order model that explains their behavior in the case of the metal-ammonia solutions. This model shows that the resonant frequency is a (microscopic) chemical and not a (macroscopic) physical phenomenon, and that it appears to be associated with a particular species in the metal-ammonia solution. Therefore, these types of solutions are the ideal test-bed for the understanding and development of chemically tuned radiofrequency resonant materials in the bulk.

It is proposed that the next phase of this project begin with a series of further chemical experiments focused on understanding the make-up of the resonant species and the parameters that control its response. Alkali metals larger than lithium (such as sodium and potassium) will change the size and geometry of the metal-ammonia clusters without dramatically altering the ionic conductivity of the solution. The use of bivalent metals such as Calcium should result in much more rigid clusters than are formed with the alkali metals. One or both of these changes should lead to a detectable shift in the resonant frequency. In addition to varying the chemical parameters, we will need to evaluate these solutions more rapidly and over a broader band of frequencies than we did in this project. Taking the lesson learned from the lost-power curves (Figures 1 and 8), we propose a free-space reflection measurement form a disk shaped sample of the solutions. By selecting the polarization and angle of incidence properly, a sudden increase in the imaginary part of the solutions will result in a measurable change in the total power reflected from the surface. The goal would be to implement a 2-18 GHz S21 measurement that will give us real-time feedback on the presence (and location on the frequency axis) of the desired resonances as a function of chemistry. Automation of a rigorous multi-parameter fit to the working model of the permittivity will also be needed to speed up the evaluation of the different solutions.

The results of these chemistry experiments should yield a robust model for these liquid systems that will allows us to define the characteristics responsible for their radiofrequency resonances. Based on this information we can then proceed with the original proposed plan to find new systems and materials that exhibit the same behavior in the solid form. The additional chemistry experiments will also help in defining the best candidate system for the creation of the metal-ammonia xerogel as a potential resonant solid.

6.0 List of all publications and technical reports
(None)

7.0 List of participating scientific personnel
Professors and Research Professionals: Rodolfo E. Díaz, William Glaunsinger, Michael McKelvy, David Wright.
Students: Kiatkamon Iamphungporn (Received his BSEE while working on this project).

8.0 Report of Inventions
(None)

9.0 Bibliography

[1] Kiriazidou, S. A., Diaz, R. E., Alexopoulos, N. G., "Rayleigh Analysis of Novel Dense Medium Exhibiting Narrow-Band Transparency Window", *IEEE Trans. Antennas and Propagation,* vol.48, no.1; Jan. 2000; p.107-16.

[2] Breitschwerdt, K. G. and Schmidt W., "Microwave Resonant absorption in metal-ammonia solutions", *Physics Letters*, vol. 50A (6), p.423ff., 1975.
[3] Mahaffey, D. W. and Jerde, D. A., "Microwave dielectric constants of sodium-ammonia solutions", *Reviews of Modern Physics*, vol. 40 (4), pp. 710-713, 1968.
[4] Marcuvitz, N., Waveguide Handbook,IEE Electromagnetic Waves Series, Peter Peregrinus Ltd., London, 1993 (Section 5.12).
[5] Breitschwerdt, K. G. and Schmidt W., "Electronic and ultrasonic properties of metal-ammonia slutionsPermittivity and dielectric relaxation in liquid-ammonia solutions"
[6] Diaz, R. E., Merrill, W. M. , Alexopoulos, N. G., "Analytic framework for the modeling of effective media", Journal of Applied Physics, vol. 84 (12),6815-6826., 1998.